Electronic Supplementary Information

A novel P2-$Na_{0.6}Li_{0.11}Fe_{0.27}Mn_{0.62}O_2$ cathode with oxygen redox reaction for high-energy Na-ion batteries

Ming-Hui Cao*[a,b], Ren-Yan Li [a], Shi-Ya Lin [a], Shao-Di Zheng [a], Lu Ma [c], Sha Tan [d], Enyuan Hu [d], Zulipiya Shadike*[e], Xiao-Qing Yang*[d] and Zheng-Wen Fu*[b]

[a] Jiangxi Province Key Laboratory of Polymer Micro/Nano Manufacturering and Devices, East China University of Technology, Nanchang, 330013, China

E-mail: mhcao@ecut.edu.cn

[b] Shanghai Key Laboratory of Molecular Catalysis and Innovative Materials, Department of Chemistry, Fudan University, Shanghai, 200433, P. R. China

E-mail: zwfu@fudan.edu.cn

[c] National Synchrotron Light Source II, Brookhaven National Laboratory, Upton, NY, 11973, USA

[d] Chemistry Division, Brookhaven National Laboratory, Upton, NY 11973, USA

E-mail: xyang@bnl.gov

[e] Institute of Fuel Cells, School of Mechanical Engineering, Shanghai Jiao Tong University, Shanghai, 200240, China

E-mail: zshadike@sjtu.edu.cn

Table S1. Stoichiometry from inductively coupled plasma-atomic emission spectrometry (ICP-AES) results of NLFMO.

Elements	Content(mg/kg)	mol ratio
Na	14.70	0.59(7)
Li	0.81	0.10(8)
Fe	16.28	0.27(4)
Mn	36.30	0.61(8)

Table S2. Refined crystallographic parameters by Rietveld analysis for NLFMO. S.G. *P63/mmc*, $a = b$ = 2.84(2) Å, c = 10.87(2) Å, $\alpha = \beta$ = 90°, γ = 120°, R_{wp}=9.72%, χ^2 = 0.6265.

Atom	Site	*x*	*y*	*z*	Occupancy	Uiso
Na1	2*d*	1/3	2/3	3/4	0.303(3)	2.3(3)
Na2	2*b*	0	0	1/4	0.297(2)	2.3(3)
Li	2*a*	0	0	0	0.114(1)	1
Fe	2*a*	0	0	0	0.268(8)	0.34(7)
Mn	2*a*	0	0	0	0.62	0.35(6)
O	4*f*	1/3	2/3	0.0872	1	0.89(88)
P63/mmc : $a = b$ = 2.8420(8) Å c =10.8722(4) Å V= 75.940(2) Å^3						
R_p = 5.70% R_{wp} =9.72% GOF(χ^2) = 0.6265						

Rietveld refinement was conducted using hexagonal space group P63/mm and by placing Mn, Fe, Li ions in octahedral sites of the transition-metal layer and Na ions at the two trigonal prismatic sites in the alkaline metal layer. The refinement shows excellent goodness of fit with this model (GOF(χ^2) = 0.6265), which confirms the proposed structural model. The similar structural model was also reported in P2-$Na_{0.66}Li_{0.18}Fe_{0.12}Mn_{0.7}O_2$ cathode material. [S1]

Table S3. Comparison of the electrochemical properties of layered cathode materials for sodium ion batteries based on anionic redox.

	Electrode materials	Voltage range (V)	Initial reversible capacity (mAh/g)	Reference
Li-doping	P2-$Na_{0.6}Li_{0.2}Mn_{0.8}O_2$	2.0-4.6	162(0.067C)	S2
	P3-$Na_{0.6}Li_{0.2}Mn_{0.8}O_2$	2.0-4.5	123(0.1C)	S3
	P2-$Na_{0.72}Li_{0.24}Mn_{0.76}O_2$	1.5-4.5	270(0.05C)	S4
	P2-$Na_{0.66}Li_{0.18}Fe_{0.12}Mn_{0.7}O_2$	1.5-4.5	214(0.05C)	S1
	P2-$Na_{0.66}Li_{0.22}Ru_{0.78}O_2$	1.5-4.5	158(0.1C)	S5
	P2-$Na_{0.75}Li_{0.2}Mg_{0.05}Al_{0.05}Mn_{0.7}O_2$	1.5-4.5	245(0.05C)	S6
	P2-$Na_{0.72}Li_{0.24}Ti_{0.1}Mn_{0.66}O_2$	1.5-4.5	194(0.05C)	S7
Mg-doping	P2-$Na_{2/3}Mg_{0.28}Mn_{0.72}O_2$	2.0-4.5	150(0.1C）	S8
	P3-$Na_{2/3}Mg_{1/3}Mn_{2/3}O_2$.	1.5-4.5	225(0.1C)	S9
	P2-$Na_{0.7}Mn_{0.6}Ni_{0.2}Mg_{0.2}O_2$	1.5-4.2	130(0.2C)	S10
Zn-doping	P2-$Na_{2/3}[Zn_{0.3}Mn_{0.7}]O_2$	1.5-4.6	190(0.1C)	S11
	P2-$Na_{2/3}[(Ni_{0.5}Zn_{0.5})_{0.3}Mn_{0.7}]O_2$	2.3-4.6	103(0.1C)	S12
Vacancy-doping	$Na_{4/7}[Mn_{6/7}(\square_{Mn})_{1/7}]O_2$	1.5-4.4	220(0.1C)	S13
	P2-$Na_{0.78}Ni_{0.23}Mn_{0.69}O_2$	2.0-4.5	138(0.1C)	S14
	$Na_{4/7-x}[\square_{1/7}Mn_{6/7}]O_2)$	1.5-4.7	200(0.05C)	S15
	P2-$Na_{2/3}Ni_{1/3}Mn_{2/3}O_2$	1.5-4.5	228(0.05C)	S16
	P2-$Na_{0.67}Cu_{0.28}Mn_{0.72}O_2$	2.0-4.5	104(0.1C)	S17

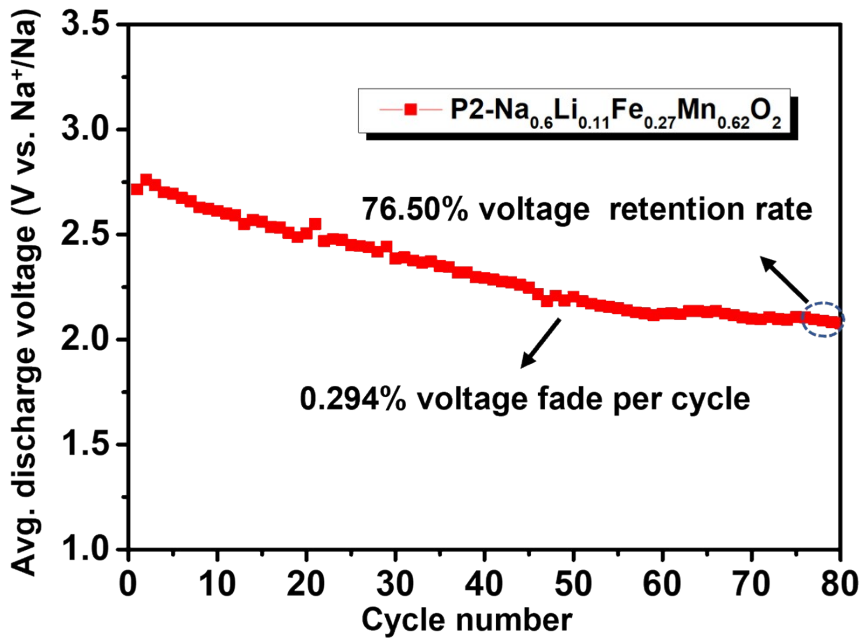

Figure S1. Average discharge voltage vs. cycle number plot of P2-NLFMO.

The average discharge voltages are plotted against cycle numbers and shown in **Figure S1**. It can be seen that the average discharge voltage decreases from 2.7154 to 2.0774 V (ΔE=0.638 V) with a voltage retention rate as 76.50% after 80 cycles for P2-$Na_{0.6}Li_{0.11}Fe_{0.27}Mn_{0.62}O_2$, indicating a serious voltage decay.

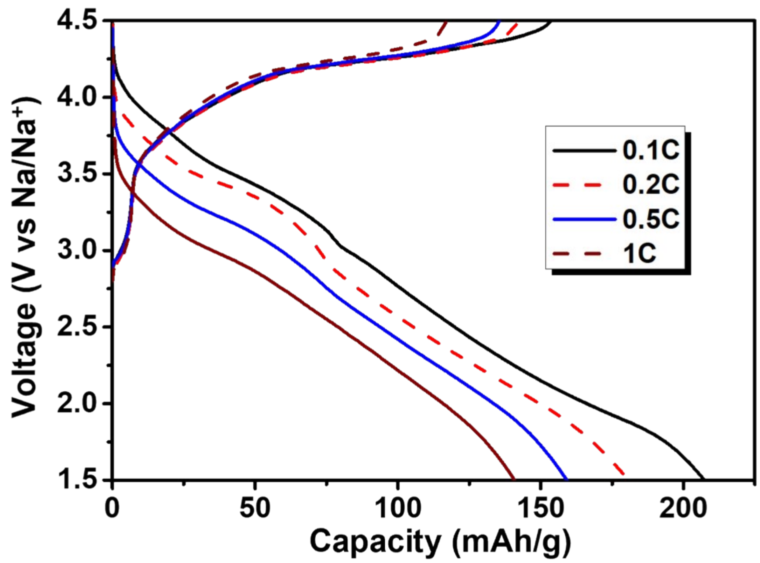

Figure S2. The charge and discharge voltage profiles with different current rate (0.1C-1C) for P2-NLFMO in Na half-cells.

Figure S2 shows the charge and discharge voltage profiles with different current rate (0.1C-1C) for P2-NLFMO in Na half-cells. It can be seen that the $Na_{0.6}Li_{0.11}Fe_{0.27}Mn_{0.62}O_2$ electrode exhibits the average discharge voltage of 2.7154, 2.6888, 2.6872 and 2.6078 V at C/10, C/5, C/2 and 1C rates, respectively. The result indicates that a severe voltage decay is the main factor leading to the poor rate capability of P2-NLFMO.

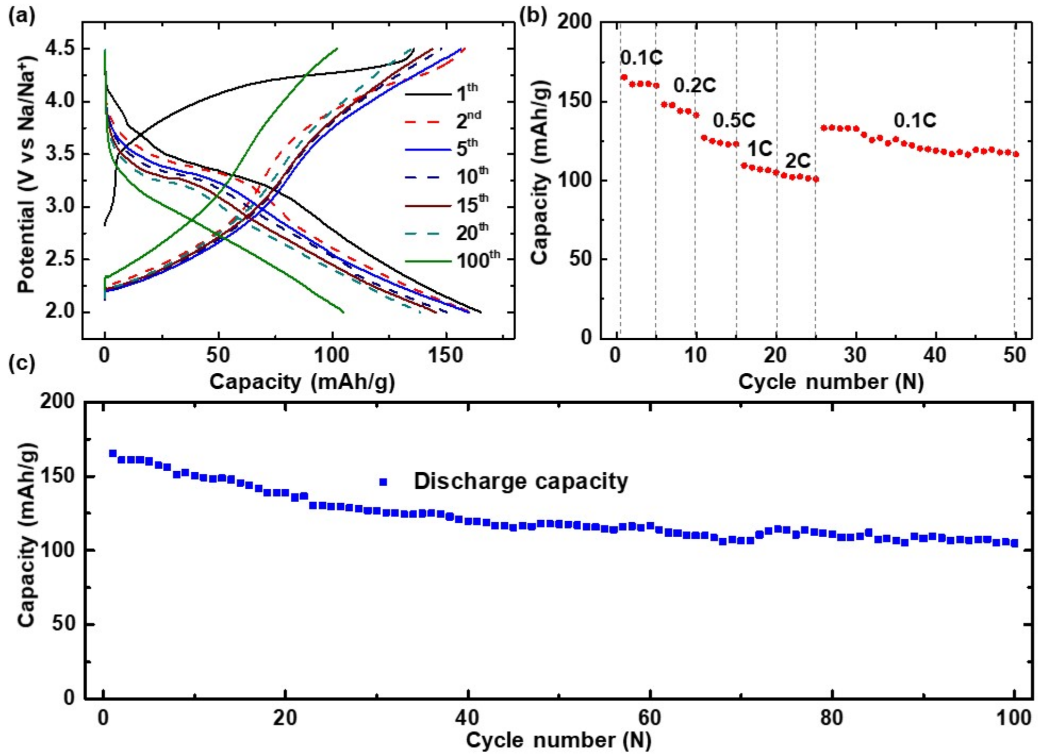

Figure S3. (a) Representative charge/discharge curves at 0.1C in the voltage range of 2.0-4.5 V, (b) Rate capability (0.1C-1C), (c) Charge/discharge capacity and Coulombic efficiency as a function of cycle number.

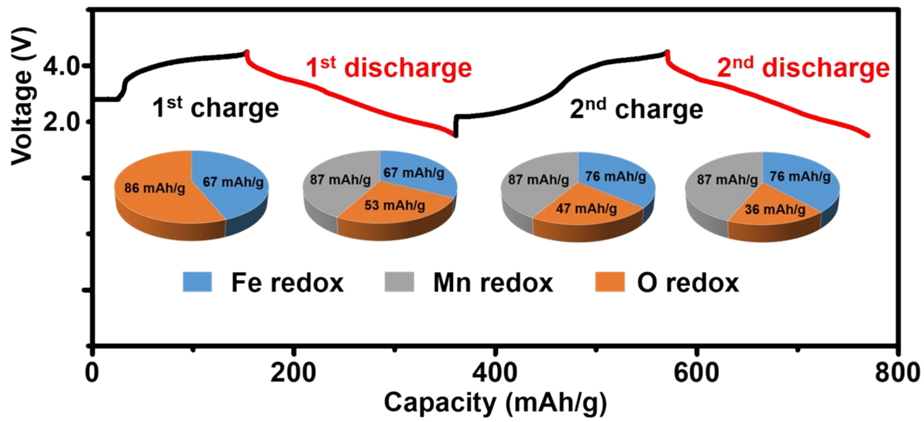

Figure S4. The capacity contributions of Fe redox, Mn redox and oxygen redox during the initial two cycles.

References

[S1] L. Yang, X. Li, J. Liu, S. Xiong, X. Ma, P. Liu, J. Bai, W. Xu, Y. Tang, Y. -Y. Hu, M. Liu and H. Chen, *J. Am. Chem. Soc.*, 2019, **141**, 6680-6689.

[S2] E. de la Llave, E. Talaie, E. Levi, P. K. Nayak, M. Dixit, P. T. Rao, P. Hartmann, F. Chesneau, D. T. Major, M. Greenstein, D. Aurbach and L. F. Nazar, *Chem. Mater.*, 2016, **28**, 9064-9076.

[S3] K. Du, J. Zhu, G. Hu, H. Gao, Y. Li and J. B. Goodenough, *Energy Environ. Sci.*, 2016, **9**, 2575-2577.

[S4] X. Rong, E. Hu, Y. Lu, F. Meng, C. Zhao, X. Wang, Q. Zhang, X. Yu, L. Gu, Y. -S. Hu, H. Li, X. Huang, X. -Q. Yang, C. Delmas and L. Chen, *Joule*, 2019, **3**, 503-517.

[S5] X. Cao, H. Li, Y. Qiao, X. Li, M. Jia, J. Cabana and H. Zhou, *Adv. Energy Mater.*, 2020, **10**, 1903785.

[S6] X. Chen, C. Cheng, M. Ding, Y. Xia, L. Y. Chang, T. S. Chan, H. Tang, N. Zhang and L. Zhang, *ACS Appl. Mater. Interfaces*, 2020, **12**, 43665-43673.

[S7] C. Li, C. Zhao, B. Hu, W. Tong, M. Shen and B. Hu, *Chem. Mater.*, 2020, **32**, 1054-1063.

[S8] U. Maitra, R. A. House, J. W. Somerville, N. Tapia-Ruiz, J. G. Lozano, N. Guerrini, R. Hao, K. Luo, L. Jin, M. A. Pérez-Osorio, F. Massel, D. M. Pickup, S. Ramos, X. Lu, D. E. McNally, A. V. Chadwick, F. Giustino, T. Schmitt, L. C. Duda, M. R. Roberts and P. G. Bruce, *Nature Chem.*, 2018, **10**, 288-295.

[S9] B. Song, E. Hu, J. Liu, Y. Zhang, X. Q. Yang, J. Nanda and K. Page, *J. Mater. Chem. A*, 2019, **7**, 1491-1498.

[S10] Q. C. Wang, J. K. Meng, X. Y. Yue, Q. Q. Qiu, Y. Song, X. J. Wu, Z. -W. Fu, Y. -Y. Xia, Z. Shadike, J. Wu, X. -Q. Yang and Y. N. Zhou, *J. Am. Chem. Soc.*, 2018, **141**, 840-848.

[S11] A. Konarov, J. H. Jo, J. U. Choi, Z. Bakenov, H. Yashiro, J. Kim and S. T. Myung, *Nano energy*, 2019, **59**, 197-206.

[S12] A. Konarov, H. J. Kim, J. H. Jo, N. Voronina, Y. Lee, Z. Bakenov, J. Kim and S. T. Myung, *Adv. Energy Mater.*, 2020, **10**, 2001111.

[S13] Y. Li, X. Wang, Y. Gao, Q. Zhang, G. Tan, Q. Kong, S. Bak, G. Lu, X. -Q. Yang, L. Gu, J. Lu, K. Amine, Z. Wang and L. Chen, *Adv. Energy Mater.*, 2019, **9**, 1803087.

[S14] C. Ma, J. Alvarado, J. Xu, R. J. Clément, M. Kodur, W. Tong, C. P. Grey and Y. S. Meng, *J. Am. Chem. Soc.*, 2017, **139**, 4835-4845.

[S15] B. Mortemard de Boisse, S. I. Nishimura, E. Watanabe, L. Lander, A. Tsuchimoto, J. Kikkawa, E. Kobayashi, D. Asakura, M. Okubo and A. Yamada, *Adv. Energy Mater.*, 2018, **8**, 1800409.

[S16] T. Risthaus, D. Zhou, X. Cao, X. He, B. Qiu, J. Wang, L. Zhang, Z. Liu, E. Paillard, G. Schumacher, M. Winter and J. Li, *J. Power Sources*, 2018, **395**, 16-24.

[S17] W. Zheng, Q. Liu, Z. Wang, Z. Wu, S. Gu, L. Cao, K. Zhang, J. Fransaer and Z. Lu, *Energy Storage Mater.*, 2020, **28**, 300-306.